PERGAMON

Aerosol Science 34 (2003) 1399–1420

Journal of
Aerosol Science

www.elsevier.com/locate/jaerosci

Carbon mass determinations during the AIDA soot aerosol campaign 1999

H. Saathoff[a,*], K.-H. Naumann[a], M. Schnaiter[a], W. Schöck[a], E. Weingartner[b], U. Baltensperger[b], L. Krämer[c], Z. Bozoki[c], U. Pöschl[c], R. Niessner[c], U. Schurath[a]

[a] *Institut für Meteorologie und Klimaforschung, Forschungszentrum Karlsruhe, Postfach 3640, D-76021 Karlsruhe, Germany*
[b] *Laboratory of Atmospheric Chemistry, Paul Scherrer Institute, 5232 Villigen, Switzerland*
[c] *Institute of Hydrochemistry, Technical University of Munich, Marchioninistrasse 17, D-81377 Munich, Germany*

Received 30 July 2002; accepted 24 April 2003

Abstract

During the soot aerosol campaign particle carbon mass concentrations of Diesel soot, spark generated "Palas" soot, external and internal mixtures of Diesel soot with $(NH_4)_2SO_4$, and particles coated with secondary organic aerosol material were determined by several different methods. Two methods were based on thermochemical filter analysis with coulometric and NDIR detection of evolved CO_2 (total carbon, TC and elemental carbon, EC) and four methods employed optical techniques: aethalometry (black carbon, BC), photoacoustic soot detection (BC), photoelectron emission, and extinction measurement at 473 nm. Furthermore, β-attenuation (total particulate mass), FTIR spectroscopy (sulphate), and COSIMA model calculations were used to determine particle mass concentrations. The general agreement between most methods was good although some methods did not reach their usual performance. TC determined by coulometric filter analysis showed good correlations with optical extinction, photoacoustic BC signal, and photoelectron emission data. However, the evolution of the photoelectron emission signal correlated with changes in accessible surface area rather than mass concentration and was very sensitive to surface conditions. The BC content as measured by the aethalometers approximately equal to less than 70% of the EC content for Diesel soot and amounts to less than 25% of the EC content of "Palas" soot.

Keywords: Soot mass determination; Elemental carbon; Black carbon

* Corresponding author. Tel.: +49-7247-82-2897; fax: +49-7247-82-4332.
E-mail address: harald.saathoff@imk.fzk.de (H. Saathoff).

0021-8502/$ - see front matter © 2003 Elsevier Ltd. All rights reserved.
doi:10.1016/S0021-8502(03)00365-3

1. Introduction

Carbon containing particles are an important fraction of the atmospheric aerosol (Penner & Novakov, 1996). They influence the global radiation budget especially by absorbing light and by acting as cloud condensation nuclei (IPCC, 2001). The mean atmospheric residence time of these particles ranges from 6 to 10 days (Cooke & Wilson, 1996). Therefore, their spatial distribution is highly inhomogeneous and strongly correlated with their sources (Lavanchy, Gäggeler, Schotterer, Schwikowski, & Baltensperger, 1999b; Raes et al., 2000). Whereas biomass burning is the dominant source in tropical and savannah regions, most of the fossil fuel is combusted at mid-latitudes (Liousse et al., 1996; Cooke & Wilson, 1996; Cooke, Liousse, Cachier, & Feichter, 1999). The most common parameter to quantify carbonaceous aerosol is its carbon mass. Usually three carbonaceous fractions are distinguished: organic carbon (OC), black or elemental carbon (BC or EC), and inorganic carbon (e.g. carbonates). Furthermore, the nomenclature for the description of carbonaceous particles uses: total carbon (TC = EC + OC), non-extractable carbon (NEC), non-volatilisable carbon (NVC), and others (e.g. Petzold & Niessner, 1995). These terms are related to the methods used for analysis of aerosol samples rather than to the origin of the respective particulate matter. Incomplete combustion of carbon containing fuels leads to the formation of particles with a graphitic microstructure that is strongly light absorbing. These compounds are therefore called BC or also EC. According to the particle formation mechanism during combustion, the "graphitic" nucleus of a combustion particle is covered with organic compounds (Petzold & Niessner, 1995). Soot is therefore composed of "elemental" and "organic" carbon (Moosmüller et al., 2001). Unfortunately, the specific attenuation cross section of BC is not well defined: a range of 2–25 $m^2\ g^{-1}$ is quoted in the literature (Liousse, Cachier, & Jennings, 1993). One reason for this order of magnitude range is the often-neglected wavelength dependence of the absorption (Moosmüller et al., 1998). Another reason lies in the different methods for EC determination, which yield widely differing results (Schmid et al., 2001). BC denotes that part of the carbonaceous aerosol, which strongly absorbs visible light. Its mass fraction in ambient aerosols is assumed to be approximately equal to that of EC which is defined by its thermochemical behaviour: it does not volatilise in an inert atmosphere at temperatures as high as 650°C, and can only be gasified by oxidation which starts at temperatures above 340°C in pure oxygen (Cachier, Bremond, & Buat-Ménard, 1989; Petzold & Niessner, 1995; Lavanchy, Gäggeler, Nyeki, & Baltensperger, 1999a). Organic particulate matter is either directly emitted into the atmosphere (primary organics), or results from reactions of volatile organic precursors in the gas phase. Both the primary and secondary organic matter may condense on pre-existing particles or form new particles by homogeneous nucleation (Baltensperger et al., 2002). Depending on the emission source, the EC core of combustion particles is covered with more or less volatile material. These coatings can have a significant influence on the optical and hygroscopic particle properties.

Today most measurement techniques for atmospheric carbonaceous particles are based on the initial sampling of the aerosol particles on filters. This initial step is followed by analysis of the filter load by methods like extraction, thermography, coulometry, etc. (Schmid et al., 2001; VDI, 1996, 1999), or by optical methods (e.g. aethalometer, integrating plate, etc.). Some of these methods allow for continuous measurements, e.g. by using a moving filter tape. Other methods like photoacoustic soot detection are less common in atmospheric applications. OC is usually equated to carbonaceous material that is gasified by low-temperature oxidation or volatilisation in an inert gas atmosphere (VDI, 1999). Some analysis methods combine liquid extraction and thermal desorption to determine

the OC and EC fractions (VDI, 1996). Other methods combine for this purpose thermal sample treatment with optical transmission (Birch & Cary, 1996) or reflectance measurements (Chow et al., 1993). TC methods are usually based on the complete oxidation of OC and EC and detection of the CO_2 evolved.

During the present soot aerosol investigation, the following methods were applied to determine aerosol mass concentrations: Samples collected on quartz fibre filters were analysed for TC with the coulometric method, and for OC and EC by thermography (Lavanchy et al., 1999a). Total aerosol mass concentration was determined with a betameter. The method is based on continuous measurement of β-attenuation by particles, which are collected on a filter tape. Two different aethalometers were used to measure light attenuation by soot-loaded filter tapes. Furthermore, a new photoacoustic sensor (Krämer, Bozoki, & Niessner, 2001) was used for BC monitoring. For those experiments with pure soot aerosol, the soot mass concentration was also calculated from measured extinction values using the specific soot extinction cross sections determined by Schnaiter et al. (2003). The photoelectron emission from soot particles was measured and used for soot mass determinations where appropriate. Additionally, the evolution of the soot mass concentration was calculated with the COSIMA aerosol model (Naumann, 2003) using the initially measured particle size distributions and number concentrations for initialisation.

Several intercomparison exercises of different soot measurement methods have been reported in the literature (e.g. Schmid et al., 2001; Hitzenberger et al., 1999; Petzold & Niessner, 1995; Hansen & Novakov, 1990). Work reported in this paper focuses on a different task, namely on the *consistency* of carbon mass measurements (and of $(NH_4)_2SO_4$ mass measurements, as appropriate), to furnish a reproducible basis for the simultaneously measured optical and other relevant aerosol properties. Therefore, the concentrations used were much higher than for example in the urban atmosphere. The campaign offered an opportunity to apply the above-described techniques to aerosols, which differed by composition or by state of mixing in a well-defined manner. Because of their relevance for BC measurements in atmospheric samples, the results of the aethalometer measurements are analysed in more detail in a separate paper (Weingartner et al., 2003).

2. Experimental and modelling

The AIDA[1] aerosol chamber and other relevant equipment were described by Saathoff et al. (2003b). Carbon mass determinations of dilute Diesel soot aerosol from a VW 4 cylinder turbo Diesel engine, and of artificial soot aerosol ("Palas" soot) from a commercial spark discharge generator (GfG 1000, Palas) which was run with pure argon, were carried out during a series of experiments in the AIDA chamber. The "Palas" soot aerosol was used without further purification, while the Diesel soot aerosol was passed through molecular sieve, activated carbon, and cobalt oxide denuders to reduce the amounts of water vapour, volatile organics, and NO_x present in the aerosol (Arens, Gutzwiller, Baltensperger, Gäggeler, & Ammann, 2001). Due to the long lifetime of soot aerosol in the 84 m^3 chamber with respect to sedimentational and diffusional losses, it was possible to utilise direct and indirect methods simultaneously to measure or monitor carbon mass in the chamber on time scales of days. Effects of aerosol ageing, oxidation by ozone, coating with oxidation products of

[1] Aerosols, Interactions and Dynamics in the Atmosphere.

α-pinene, and external/internal mixing with ammonium sulphate could thus be studied in considerable detail. Model-calculated time dependencies of soot aerosol mass, size distribution, and surface area in the AIDA chamber were provided by the COSIMA code for fractal aerosols, for comparison with the experimental data. The model takes account of dilution effects that arise from the various sampling instruments. The COSIMA code and its optical module are described in detail by Naumann (2003). Relevant experimental techniques are briefly described in the following sections.

2.1. Filter sampling and analysis

Soot aerosol for carbon analysis was sampled on preheated (250°C) quartz fibre filters (∅47 mm, MK 360, Munktell) at flow rates between 5 and 10 l min^{-1} via stainless steel tubes (i.d. 4 or 8 mm), which protruded 400 mm into the AIDA chamber. Before adding soot aerosol to the chamber, clean chamber air was sampled in each experiment to provide filter blanks for background subtraction. The TC values obtained for these filter blanks had an average value of (65 ± 20) $(\pm 2\sigma)$ μg Cm^{-3}. Their variability determines the uncertainty of the TC analysis.

The TC determinations served as reference for several other more indirect methods. They were carried out with a commercial carbon analyser (Coulomat 702, Ströhlein), similar to the instrument described by VDI (1996), which was routinely calibrated with weighted samples of anhydrous $CaCO_3$. The loaded filters were heated in pure O_2 gas (flow rate 2.3 l min^{-1}) from room temperature to 900°C within 20 s. The carrier gas passed on through a CuO/Pt oxidation catalyst at 800°C and through silver wool at 600°C. The evolved CO_2 was determined by automated coulometric titration. The detection limit for the coulometric TC analysis is limited by the variation of the unloaded blank filter values. Despite of the described pre-treatment these values averaged at (13 ± 7) $(\pm 2\sigma)$ μg C for quartz fibre filters of 47 mm diameter. After the campaign, the TC analyser was additionally equipped with an NDIR CO_2 monitor (MLT 1.1, Fisher-Rosemount). This fast detector was used for time-resolved measurements of CO_2 formation while filter samples were rapidly heated, first from room temperature to 340°C, and after 10 min from 340°C to 650°C.

Furthermore, aerosols were sampled on prefired (800°C) quartz fibre filters (∅25 mm, Schleicher & Schüll), and analysed for OC and EC using the thermal method of Lavanchy et al. (1999a). OC was determined by rapidly heating the filter samples to 340°C in pure O_2, and maintaining this temperature for 42 min. Subsequently, the temperature was rapidly raised and maintained at 650°C for another 32 min to determine EC. In both cases the O_2 carrier gas passed through a CuO catalyst at 950°C to oxidise volatile organics and CO to CO_2, which was collected in molecular sieve traps. The traps were rapidly heated to 200°C, and the evolving CO_2 was determined by NDIR. However, the filters adsorbed varying amounts of gaseous OC both from the chamber background and from the gaseous products of the ozonolysis of α-pinene. Therefore, the OC values determined are not reported. Where appropriate, additional aerosol samples were collected on Teflon filters and analysed for anions and cations by ion chromatography (DX-500, Dionex). The detection limit for sulphate was 0.02 mg l^{-1}.

2.2. Optical methods

Aerosol for optical analysis was sampled via stainless steel tubes as described in Section 2.1. Two home-made instruments for monochromatic/polychromatic extinction measurements and a

commercial nephelometer (3563, TSI) were connected in series to the same sampling line. The line was periodically switched between soot aerosol and filtered particle-free air from the AIDA chamber for background subtraction, as described by Schnaiter et al. (2003). Two aethalometers, a betameter, and a photoelectron emission sensor were connected to another sampling manifold. This line was periodically switched between chamber aerosol and filtered laboratory air for background subtraction. The latter was used to minimise aerosol depletion in the chamber, in view of the high flow rates required by this set of instruments. Another sampling line provided chamber air for photoacoustic soot monitoring.

Aerosol extinction spectra covering the wavelength range 230–1000 nm were measured along a flow tube of 5 m length, using a deuterium/halogen lamp combination (DH-2000-FHS, Avantes), fibre optics, and diode array spectrometers (MCS 55, Zeiss). More sensitive extinction measurements were made with a multiple reflection cell (75 m optical path) which incorporated a 473 nm LED (spectral band width 35 nm) as light source. The total aerosol particle scatter and backscatter cross sections were determined at 450, 550 and 700 nm with an integrating nephelometer (3563, TSI). Mass-specific extinction, scattering, and absorption cross sections were deduced at these wavelengths by combining TC analysis (see above) with the obtained optical data, as described in detail by Schnaiter et al. (2003). Extinction measurements at 473 nm with the multiple reflection cell were also used to interpolate TC mass concentrations of pure soot aerosols in the AIDA chamber between filter samplings. The specific extinction cross sections of $(10.2 \pm 0.4)\ m^2\ g^{-1}$ (Diesel soot) and $(5.6 \pm 0.2)\ m^2\ g^{-1}$ (Palas soot) were taken from Schnaiter et al. (2003).

Two different aethalometers were run simultaneously to measure the wavelength-dependent absorption coefficient as well as the BC concentration during chamber experiments, as described in detail by Weingartner et al. (2003). The standard instrument (AE10, MAGEE Scientific) incorporated an incandescent lamp, which emits a broad continuous spectrum. The other instrument (AE30, MAGEE Scientific) was a prototype that measured light attenuation by BC at 450, 590, 615, 660, 880, and 950 nm simultaneously. These wavelengths are emitted by a set of solid-state sources with typical spectral bandwidths of 20 nm. With this instrument, BC was determined from the attenuation measurement at $\lambda = 880$ nm. BC concentrations reported in this paper are based on specific attenuation cross sections α of 16.6 and $19\ m^2\ g^{-1}$ for the AE30 and AE10, respectively, which were provided by the manufacturer. During all experiments it was observed that the measured BC values decreased with increasing particle load of the filter. Therefore, the averages BC values reported in this paper were calculated by interpolating the raw values to the mean filter light attenuation of 35% and 25% for the AE30 and AE10, respectively (see Weingartner et al., 2003 for more details).

BC concentrations were also measured with a prototype Photo-Acoustic Soot Sensor (PASS, Krämer et al., 2001). This instrument uses a 3880 Hz square-wave modulated diode laser which emits 0.25 W of 680 nm radiation to induce the acoustic signal. Before the AIDA campaign, the photoacoustic sensor had been calibrated with soot aerosol from another "Palas" generator. Even though it is known that the used "Palas" soot contains also OC, the TC as determined by coulometry, was used to determine the mass-specific absorption cross section, yielding a value of $2.7\ m^2\ g^{-1}$ and a detection limit below $1\ \mu g\ m^{-3}$. No significant interference was detected for non-absorbing aerosol at concentrations up to $1\ mg\ m^{-3}$. For consistency with the optical measurements performed during the AIDA campaign, the mass-specific absorption cross sections of "Palas" and Diesel soot reported by Schnaiter et al. (2003) were adopted here to convert the photoacoustic signals into BC

mass concentrations, which are inversely proportional to the assumed absorption cross section. The implications will be discussed below.

Soot aerosol particles exposed to 222 nm radiation in a tubular excimer lamp become positively charged due to the emission of photoelectrons. This effect is highly correlated with the amount of surface-adsorbed polycyclic aromatic hydrocarbons (Burtscher, 1992; Hüglin, Gaegauf, Künzel, & Burtscher, 1997). However, the ionisation potentials of gaseous PAHs (Lide, 1998) are significantly higher than the photon energy of the excimer lamp (5.6 eV), which is in turn higher than the work function of graphite (4.48 eV, Hansen & Hansen, 2001). Measurements were carried out with a commercial photoelectric aerosol sensor (PAS 2000, EcoChem, cf. Burtscher & Siegmann, 1994; Baltensperger, Weingartner, Burtscher, & Keskinen, 2001), which measures the photocurrent by collecting the charged soot particles on an insulated fabric filter. The signal can be used as a proxy for soot aerosol mass concentrations under properly controlled conditions (Matter, Siegmann, & Burtscher, 1999; Dahmann, Mosimann, & Matter, 2000), see also below.

During experiments with $(NH_4)_2SO_4$ aerosol, sulphate mass concentrations were measured in situ and quasi-continuously with an FTIR spectrometer (IFS 66v, Bruker, resolution 0.125 cm^{-1}), using a 254 m long folded light path inside the AIDA chamber. The integrated sulphate absorption band at 1120 cm^{-1} was compared with sulphate mass concentrations determined by ion chromatography of filter samples. The obtained integrated absorption coefficient, $B = (3.8 \pm 0.4) \times 10^3$ m g^{-1}, is in good agreement with literature data (Toon, Pollack, & Khare, 1976).

2.3. Other instruments and methods

Total aerosol mass was determined with a commercial betameter (FH 62-I-R, Eberline, cf. VDI, 1987) which collects particles on filter tape. The instrument measures attenuation of β-radiation from an ^{85}Kr source by the sampling spot and by a reference foil continuously. Since the mass attenuation coefficients of carbon and ammonium sulphate are equal (Baltensperger et al., 2001), the deposited aerosol mass was obtained independent of particle composition from the difference between the sampling spot and reference foil channels, using the calibration factor provided by the manufacturer. The instrument was operated at a flow rate of 1 m^3 h^{-1}.

To initialise the COSIMA model calculations which yield the time evolution of soot aerosol mass, size, and surface distribution, and of soot optical properties (Naumann, 2003; Wentzel, Gorzawski, Naumann, Saathoff, & Weinsbruch, 2003; Schnaiter et al., 2003), initial number densities and particle size distributions were provided for each chamber experiment with a condensation nuclei counter (CNC 3010, TSI) and a differential mobility analyser (DMA 3071, TSI). In addition to these parameters, the variable chamber dilution factors by the various sampling processes were an important input to the model calculations. Before starting an experiment, a small amount of SF_6 was injected into the chamber as an inert tracer. Frequent SF_6 measurements by FTIR spectroscopy yielded chamber dilution factors, which were in good agreement with bookkeeping data.

3. Results and discussion

For each of the 10 experiments carried out during the AIDA soot campaign, initial (i) and final (f) aerosol mass concentrations are listed in the columns of Tables 1a–1c. The introductory paper

by Saathoff et al. (2003b) should be consulted for further details. The analytical methods or instruments are listed in the first column, using the notation introduced in Section 2. During the coating experiment nos. 7–9 additional filter samples were collected when most of the α-pinene had reacted with ozone (index *m* at top of column). Note that the experimental time scales were set to zero either when all aerosol(s) had been injected into the chamber, or in the case of coating experiments after the injection of α-pinene. Hours before $t = 0$ are therefore marked with a minus sign.

Table 1a
Carbon mass concentrations determined for pure soot aerosol with various methods

Exp. no.	1*i*	1*f*	2*i*	2*f*	3*i*	3*f*
Aerosol type	"Palas" soot		Diesel soot		"Palas" soot	
Date in 1999	4 Oct.	5 Oct.	6 Oct.	8 Oct.	11 Oct.	13 Oct.
Time of sampling (h)	0.7 ± 0.4	24.5 ± 0.5	0.4 ± 0.2	43 ± 1	0.5 ± 0.3	43 ± 1
TC filter	125 ± 38	95 ± 29	67 ± 20	59 ± 18	100 ± 30	72 ± 22
EC filter	53 ± 16	42 ± 14	77 ± 20	44 ± 15	54 ± 16	69 ± 18
BC AE 10	n.a.	13 ± 2	53 ± 3	29 ± 2	19 ± 1	10 ± 1
BC AE 30	n.a.	11 ± 2	52 ± 2	22 ± 1	13 ± 1	8 ± 0.5
TC from extinction	120 ± 13	90 ± 10	72 ± 8	54 ± 6	106 ± 12	76 ± 8
BC from photoacoustic	160 ± 64[a]	115 ± 46[a]	65 ± 7	52 ± 6	112 ± 44[a]	n.a.
"TC" by photoemission	—	95 ± 19	70 ± 14	46 ± 9	n.a.	61 ± 12
Total mass (Betameter)	155 ± 95	50 ± 31	n.a.	75 ± 22	n.a.	70 ± 20

All mass concentrations in ($\mu g\ m^{-3}$); n.a. = not analysed; i/f = initial/final sampling periods.
[a]Error limits reflect the uncertainty of mass-specific absorption cross section.

Table 1b
Aerosol mass concentrations determined for $(NH_4)_2SO_4$ aerosol and its mixtures with Diesel soot

Exp. no.	4*i*	4*f*	5*i*	5*f*	6*i*	6*f*
Aerosol type	Pure $(NH_4)_2SO_4$		Diesel + $(NH_4)_2SO_4$		Diesel + $(NH_4)_2SO_4$	
Date in 1999	14 Oct.	15 Oct.	18 Oct.	19. Oct	20.Oct.	22 Oct.
Time of sampling (h)	1.0 ± 0.5	24.8 ± 0.7	0.7 ± 0.9	23.5 ± 0.2	1.2 ± 0.2	42.7 ± 0.7
TC filter	—	—	69 ± 30[a]	46 ± 30[a]	93 ± 31[a]	66 ± 23[a]
EC filter	—	—	66 ± 18	54 ± 16	108 ± 24	57 ± 17
BC AE 10	—	—	55 ± 3	33 ± 2	76 ± 4	32 ± 2
BC AE 30	—	—	42 ± 2	27 ± 1	65 ± 3	34 ± 2
TC from extinction	—	—	72 ± 8	—	—	—
BC from photoacoustic	—	—	65 ± 7	50 ± 6	84 ± 9	55 ± 6
"TC" by photoemission	—	—	n.a.	n.a.	89 ± 18	47 ± 9
Total mass (Betameter)	1130 ± 328	840 ± 244	350 ± 100	230 ± 67	2100 ± 609	1140 ± 331
$(NH_4)_2SO_4$ by IC	760 ± 80	500 ± 50	136 ± 14	103 ± 10	1500 ± 150	700 ± 70
$(NH_4)_2SO_4$ by FTIR	760 ± 110	485 ± 73	137 ± 20	98 ± 15	1390 ± 210	695 ± 104

All mass concentrations in ($\mu g\ m^{-3}$); n.a. = not analysed; i/f = initial/final sampling periods.
[a]These values have been corrected for systematic blank filter deviations.

Table 1c
Aerosol mass concentrations determined for soot, $(NH_4)_2SO_4$, and organic aerosol with various methods

Exp. no.	7*i*	7*m*	7*f*	8*i*	8*m*	8*f*	9*i*	9*m*	9*f*	10*i*	10*f*
Aerosol type	Diesel + SOA coating			$(NH_4)_2SO_4$ + SOA coating			Palas + SOA coating			Organic aerosol	
Date in 1999	25 Oct.	25 Oct.	26 Oct.	26 Oct.	26. Oct.	27 Oct.	27 Oct.	28 Oct.	28 Oct.	28 Oct.	29 Oct.
Time of sampling (h)	-1.8 ± 0.8	2.3 ± 1.2	18 ± 0.2	-1.8 ± 0.2	1.6 ± 0.3	13 ± 0.2	-1.2 ± 0.2	1.5 ± 0.2	12 ± 0.2	2 ± 0.2	12 ± 0.2
TC filter	78 ± 23	170 ± 51	104 ± 31	—	68 ± 34	27 ± 34	111 ± 34	165 ± 50	116 ± 35	85 ± 26	49 ± 15
EC filter	52 ± 16	n.a.	58 ± 17	—	n.a.	n.a.	74 ± 19	n.a.	55 ± 16	n.a.	n.a.
BC AE 10	57 ± 3	80 ± 4	60 ± 3	—	—	—	23 ± 1	33 ± 2	20 ± 1		
BC AE 30	41 ± 2	63 ± 3	52 ± 3	—	—	—	15 ± 1	25 ± 1	16 ± 1		
TC by extinction	79 ± 9	—	—	n.a.	—	—	112 ± 12	—	—	—	—
"TC" by photoemission	83 ± 17	n.a.	n.a.	—	n.a.	n.a.	—	n.a.	n.a.	—	—
Total mass (betameter)	275 ± 78	n.a.	175 ± 51	1040 ± 302	1100 ± 319	715 ± 207	80 ± 40	n.a.	220 ± 110	n.a.	n.a.
$(NH_4)_2SO_4$ by IC	—	—	—	710 ± 70	n.a.	420 ± 40	—	—	—	—	—
$(NH_4)_2SO_4$ by FTIR	—	—	—	n.a.	569 ± 85	425 ± 65	—	—	—	—	—

All mass concentrations in ($\mu g\ m^{-3}$); n.a. = not analysed; i/f = initial/final sampling periods; m = additional sampling periods.

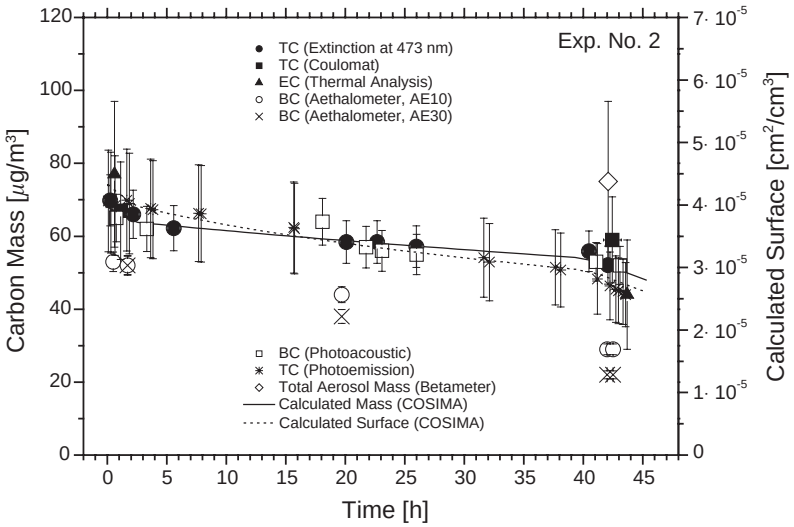

Fig. 1. Evolution of carbon mass concentrations during experiment no. 2 with pure Diesel soot.

3.1. Experiments with pure Diesel soot or pure "Palas" soot

During experiment no. 2 with pure Diesel soot and no. 3 with pure "Palas" soot, the evolution of the carbon mass concentration was monitored or calculated by up to eight different but not always independent methods. Fig. 1 depicts the slowly changing carbon mass concentration of Diesel soot aerosol in the AIDA chamber during experiment no. 2, which lasted 44 h. Mass concentrations obtained by TC analysis of filter samples, interpolated on the basis of optical extinction measurements at 473 nm, and derived from BC measurements with the photoacoustic soot sensor (PASS), are continuously in good agreement. They also agree well with the time evolution predicted by the COSIMA model. This is not surprising since the optical multipath cell and the photoacoustic instrument had both been calibrated against TC determinations by the Coulomat, while the COSIMA model was initiated with the aerosol size distribution and TC mass measured at $t = 0$. The continuously good agreement among the above methods is taken as evidence that the optical properties of soot aerosol did not change significantly during the 2 days of ageing in the AIDA chamber, in agreement with theoretical considerations, see Schnaiter et al. (2003). However, the signal of the photoemission instrument decayed somewhat faster than the signals of the other instruments and the modelled carbon mass concentration, although the sensor had been calibrated to fit the first TC analysis. The agreement is better when the photoemission signal is compared with the time evolution of the accessible soot surface area calculated by the COSIMA model. This is reasonable since the number of photoelectrons emitted far from saturation should be proportional to particle surface area rather than to particle mass, see also Niessner (1986), Burtscher (1992), and Hüglin et al. (1997). The aethalometers yielded BC mass concentrations that were between 80% and 40% of the TC measurements. The betameter was the only instrument measuring total aerosol particle mass directly. A single measurement at the end of the second day yielded a total mass concentration, which exceeded the TC measurements by about 25%, which may be due to adsorption of semivolatile components on

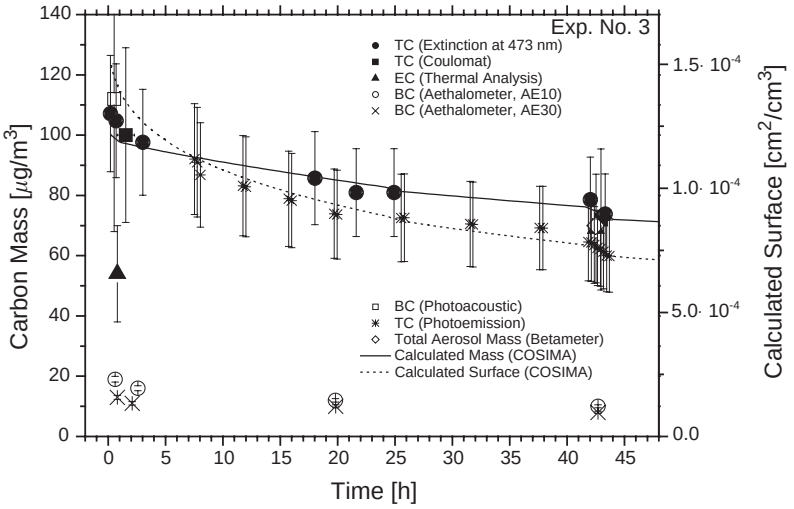

Fig. 2. Evolution of carbon mass concentrations during experiment no. 3 with pure spark generated "Palas" soot.

the filter of the betameter. Thermal analysis of filter samples collected at the beginning and at the end of experiment no. 2 yielded EC masses that agreed within error limits with the TC measurements. This is taken as evidence that the EC content of Diesel soot was high.

Fig. 2 shows the slow decay of the carbon mass concentration associated with "Palas" soot aerosol during experiment no. 3. Except for a slightly higher initial mass concentration, the experimental procedures (sampling intervals, overall duration) were similar to the Diesel soot experiment no. 2. TC analysis of filter samples and the interpolations based on optical extinction at 473 nm agreed very well amongst each other and with the COSIMA model. The only measurement by the photoacoustic sensor is in good agreement with these observations at the beginning of the experiment. This was expected since the same optical constant was applied. The decay of the photoemission signal was again in better agreement with the specific surface area of the soot aerosol which decays significantly faster than the TC mass. The sensitivities of photoemission expressed in terms of TC mass concentration, (27 ± 6) fA m^3 μg^{-1}, were about the same for Diesel and "Palas" soot. However, when expressed in terms of photocurrent per surface area concentration, the photoemission sensitivity for Diesel soot was about twice as high as for "Palas" soot, which may be due to different surface properties (Niessner, 1986; Burtscher, 1992).

The BC concentrations measured by both aethalometers were not in agreement amongst each other which is explained by the ill-defined spectral sensitivity of the AE10 instrument and by the different optical transmissions of the filters used in the two instruments (Weingartner et al., 2003). Furthermore, the BC values amounted to less than 20% of the TC mass, indicating that the absorption efficiency provided by the instrument manufacturer does not apply to "Palas" soot when referred to TC mass. In other words, the BC (i.e. the strongly light absorbing carbon) fraction in Diesel soot is large, but rather low in "Palas" soot. This is corroborated by the fact that thermal analysis of filter samples yielded significantly smaller EC than TC mass concentrations. On average (five measurements) , "Palas" soot contained ∼60% EC, with relatively large scatter. In the case of Diesel soot, the average EC content amounted to ∼95% (seven measurements). The smaller EC content of

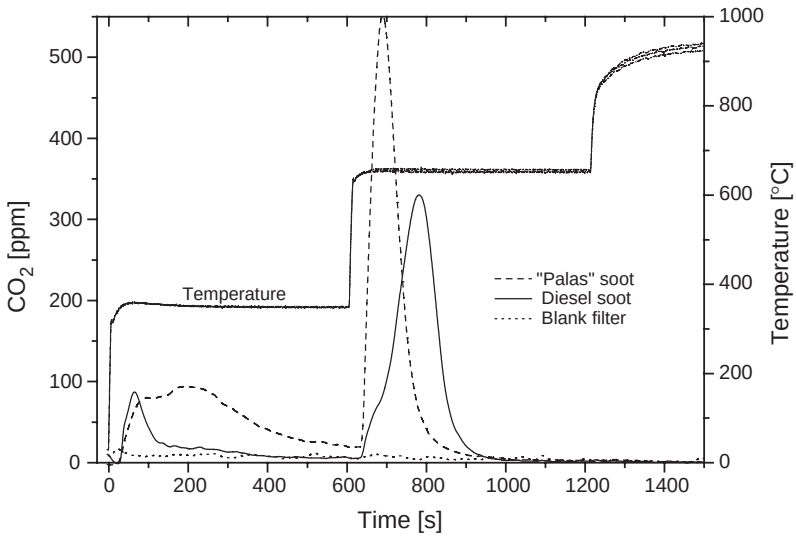

Fig. 3. Formation of carbon dioxide during thermal analysis of Diesel and "Palas" soot deposited on quartz fibre filters. This analysis was done in pure oxygen.

"Palas" soot is in qualitative agreement with measurements carried out with the TC analyser after the AIDA campaign: An NDIR CO_2 monitor was used instead of the automatic coulometric titration unit, as described in Section 2.1. It was therefore possible to obtain the time-resolved evolution of CO_2 from Diesel and "Palas" soot while following a two-step heating protocol in pure oxygen gas, as depicted in Fig. 3. Integration of the CO_2 profiles evolved at 340°C and at 650°C yielded EC contents of about 85% for Diesel soot and of about 60% for "Palas" soot. It is interesting to note that the shapes of the CO_2 recordings for Diesel and "Palas" soot are also quite different. This is not surprising in view of other profound differences between Diesel and "Palas" soot that could be disclosed by TEM, ESR and optical studies, see companion papers in this issue (Wentzel et al., 2003; Saathoff et al., 2003b; Schnaiter et al., 2003). Shortly before the end of experiment no. 3, a total aerosol mass of about 70 $\mu g\, m^{-3}$ was measured with the betameter, in good agreement with the TC measurement.

3.2. Mixtures of Diesel soot with $(NH_4)_2SO_4$ aerosol

In experiment nos. 4–6, the $(NH_4)_2SO_4$ aerosol mass concentrations determined by ion chromatography (IC) and by in situ FTIR spectroscopy were always in good agreement, see Table 1b and Figs. 4 and 5. In reference experiment no. 4 with pure dry $(NH_4)_2SO_4$ aerosol, the betameter yielded initial and final mass concentrations which were 50–70% higher than the IC and FTIR data. Total aerosol mass determined with the betameter exceeded the sum of TC + $(NH_4)_2SO_4$ mass also in experiment nos. 5 and 6. A more systematic analysis of the betameter results is presented in Section 3.4. Fig. 4 shows the evolution of the different mass concentrations during experiment no. 5 with Diesel soot and $(NH_4)_2SO_4$ aerosol. TC agreed fairly well with BC measured by the photoacoustic instrument. Also, the two extinction measurements at 473 nm before $(NH_4)_2SO_4$ was added yielded

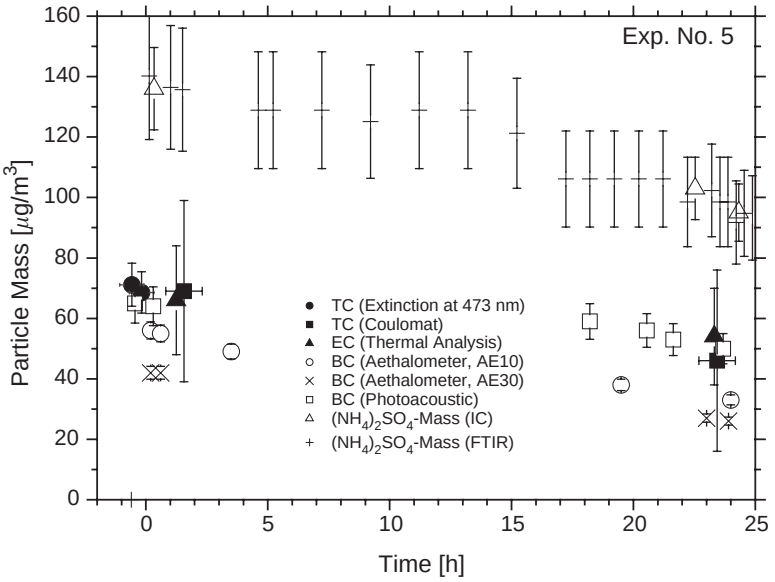

Fig. 4. Evolution of carbon and $(NH_4)_2SO_4$ mass concentrations during experiment no. 5 with a mixture of Diesel soot and $(NH_4)_2SO_4$ particles.

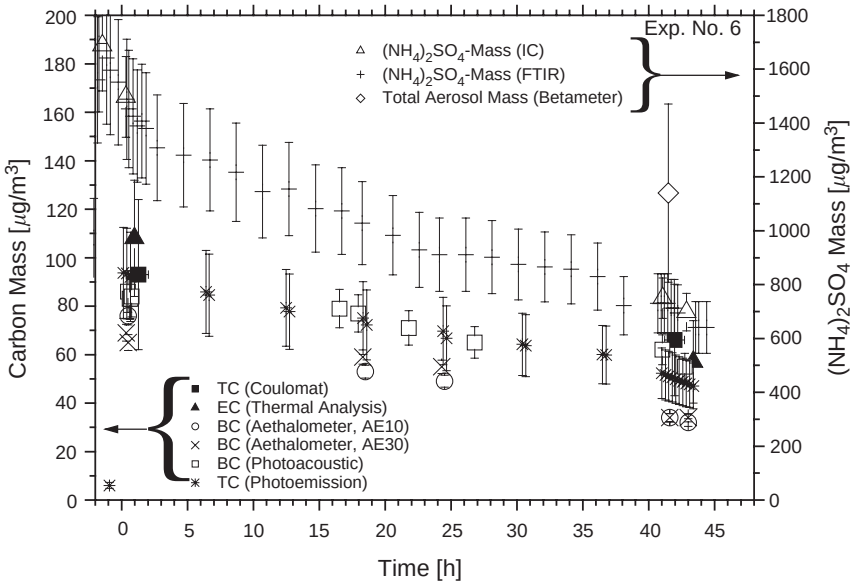

Fig. 5. Evolution of $(NH_4)_2SO_4$ and carbon mass concentrations during experiment no. 6 with a mixture of $(NH_4)_2SO_4$ and Diesel soot particles.

carbon mass concentrations in good agreement with the other data. The EC mass concentrations determined by the thermal method (Lavanchy et al., 1999a) did not differ significantly from the TC mass concentrations, confirming the result of experiment no. 2 that the EC content of Diesel soot

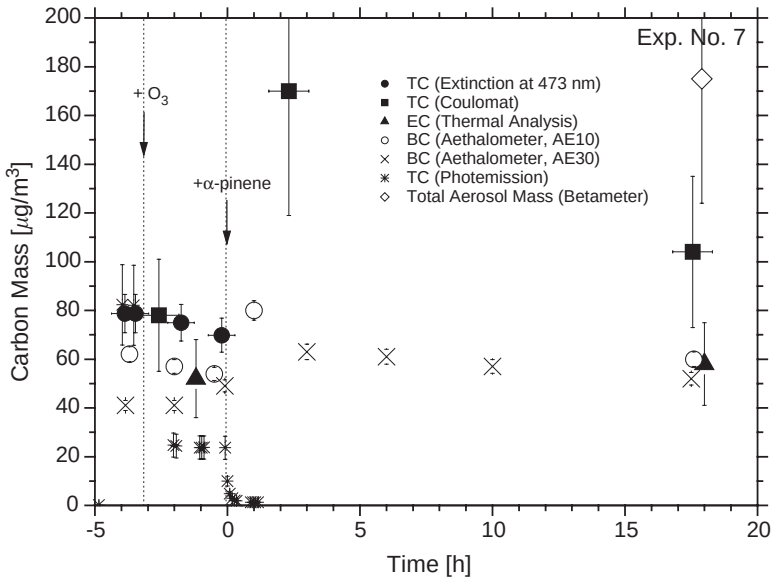

Fig. 6. Evolution of carbon mass concentrations during experiment no. 7 with Diesel soot and organic coating.

is high. Fig. 5 shows mass concentrations of $(NH_4)_2SO_4$ aerosol and carbon mass concentrations associated with Diesel soot aerosol during the 2 days of experiment no. 6 (with similar Diesel soot concentration as in experiment no. 5, but much higher $(NH_4)_2SO_4$ concentration). BC data measured by the photoacoustic instrument agreed fairly well with the photoemission measurements using the calibration factor of (27 ± 6) fA m^3 μg^{-1} introduced above. BC data from the aethalometers yielded only between 60 and 80% of these values, similar to the experiments with pure Diesel soot. The high EC content in Diesel soot was again confirmed. In summary, admixing $(NH_4)_2SO_4$ particles to Diesel soot aerosol did not affect the carbon mass determinations significantly, not even at very high concentrations.

3.3. Coating of soot and ammonium sulphate particles with secondary organic aerosol (SOA) mass

In experiment nos. 7–9, SOA mass was generated in the presence of Diesel soot, ammonium sulphate, and "Palas" soot aerosols, respectively, by injecting 61 ppb α-pinene into the chamber which contained the respective aerosol and about 500 ppb ozone. The reaction is expected to yield about 65 μg m^{-3} SOA mass (Griffin, Cocker III, Flagan, & Seinfeld, 1999) neglecting the influence of temperature (308 K compared to 297 K in this study) and relative humidity. About 64% of SOA mass is expected to be carbon (e.g., pinic acid contains 58% carbon by mass). This SOA mass may either nucleate heterogeneously on the pre-existing aerosol, thus leading to particle coating, or form new particles, or both. The coating experiments are described in detail in a companion paper by Saathoff et al. (2003a). The results of aerosol mass determinations during experiment nos. 7–9 are presented in Figs. 6–8. As in previous experiments, the total aerosol masses determined by the betameter were in large excess of the TC measurement, even when corrected for the oxygen and

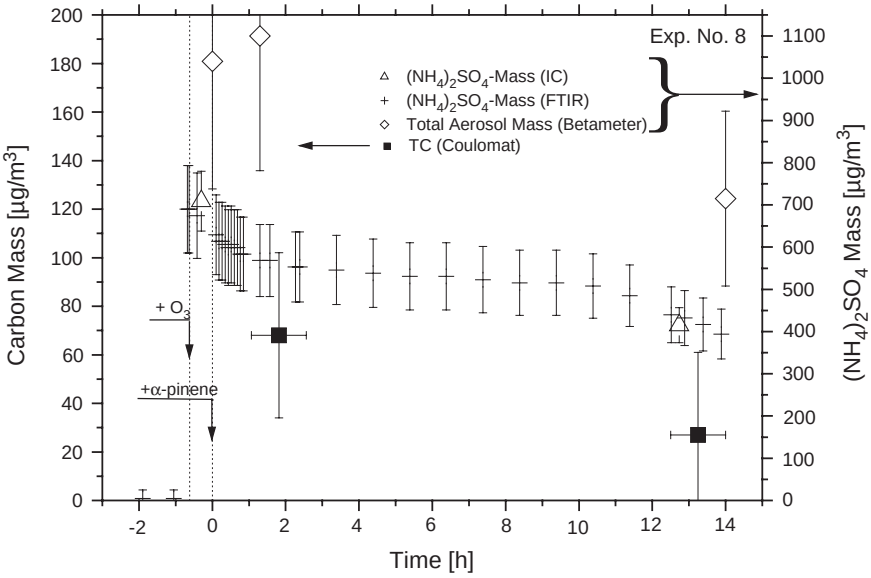

Fig. 7. Evolution of $(NH_4)_2SO_4$ and carbon mass concentrations during experiment no. 8 with $(NH_4)_2SO_4$ and organic coating.

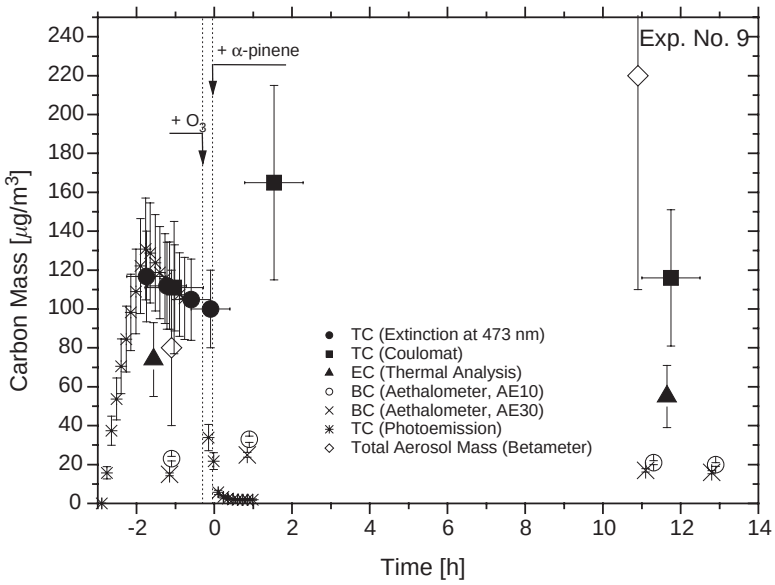

Fig. 8. Evolution of carbon mass concentrations during experiment no. 9 with "Palas" soot and organic coating.

hydrogen contents of SOA. Unfortunately, the photoacoustic instrument was not available to measure BC concentrations of the coated soot aerosols in experiment nos. 7 and 9.

Fig. 6 shows the evolution of carbon mass concentration measured before and after the coating of Diesel soot aerosol with SOA (experiment no. 7). The TC measurement after the addition of ozone,

but before α-pinene was added to the chamber, are in good agreement with the carbon masses derived from extinction measurements at 473 nm. As discussed in the companion paper by Schnaiter et al. (2003), SOA condensation strongly enhances the light scattering cross section of the coated particles. Therefore, optical extinction at 473 nm could not be used as a proxy for the BC content of coated soot aerosols. Furthermore, coating significantly affects BC measurements with the aethalometers, if comparing the values measured before and 1–3 h after the coating. The BC signal of both aethalometers increases by 40% (AE10) and 54% (AE30) upon coating, which is discussed in more detail in Weingartner et al. (2003). Aethalometer BC data was 50–70% of TC before the addition of α-pinene, as expected from experiment no. 2. TC analysis of the filter sample collected ~2 h after the addition of α-pinene yielded about twice the expected increase of ca. 42 μg m^{-3} carbon due to SOA formation. We attribute this to other less volatile products like pinonaldehyde (Yu, Cocker III, Griffin, Flagan, & Seinfeld, 1999), which are adsorbed on quartz fibre filters, giving rise to a positive interference in TC determinations (Novakov et al., 1997). The TC content measured ~18 h later was in good agreement with the estimate, indicating that the positive interference essentially disappeared with time, e.g. due to loss of the semivolatile organics to the chamber walls. It is interesting to note that the photoemission signal could be used as a proxy for TC only *before* the addition of ozone, since the signal dropped sharply by more than a factor of 3 immediately after. This is most likely due to the rapid reaction of ozone with surface functionalities and/or surface-adsorbed PAHs, as was recently reported for benzo-a-pyrene on soot aerosol by Pöschl, Letzel, Schauer, and Niessner (2001). Coating Diesel soot particles with products of the α-pinene-ozone reaction further reduces the photoemission signal to a very low level, indicating that photoelectrons cannot easily penetrate the SOA surface film. The photoemission instrument may thus also be used as a sensitive monitor for coating and other aging processes (Burtscher, Niessner, & Schmidt-Ott, 1984; Bukowiecki et al., 2002). In the same experiment after the addition of ca. 500 ppb ozone (i.e. after the oxidation of PAHs adsorbed on the Diesel soot particles), the measured EC mass amounted to roughly 2/3 of the TC mass inferred from extinction measurements at 473 nm. Unfortunately, no EC concentration had been measured before ozone was added to the Diesel soot aerosol. At 18 h after the coating event, the EC content of the coated Diesel soot aerosol amounted to about 60%.

Fig. 7 shows the results of various measurements while pure $(NH_4)_2SO_4$ aerosol was coated with ozonolysis products of α-pinene in experiment no. 8. $(NH_4)_2SO_4$ mass concentrations measured by IC and FTIR were in excellent agreement at all times. The steeper slopes of the concentration–time profiles after $t = 0$ and after $t = 11$ h are due to dilution during the sampling periods. Like in the previous coating experiment, the measured amount of 70 μg m^{-3} TC associated with the coated ammonium sulphate aerosol exceeded the expected amount of ~42 μg C m^{-3} in the SOA, while more than 10 h later a TC content of ~30 μg m^{-3} was compatible with expectations when taking into account dilution and loss.

Results of coating experiment no. 9 are shown in Fig. 8. Soot aerosol from the Palas generator was flushed into the chamber after $t = -3$ h, as indicated by the steady increase of the photoemission signal. After the aerosol generator was turned off, the photoemission signal (based on the previously determined calibration factor) was in good agreement with TC (both filter analysis and extinction measured at 473 nm). The EC content of "Palas" soot was well below the TC content, as already found in experiment no. 3. At the same time, both aethalometers yielded about a factor of 5 less BC than the TC measurements, again in agreement with experiment no. 3. Coating of "Palas" soot with SOA had a significant effect on the BC signal of the aethalometers. The BC signal of the AE10

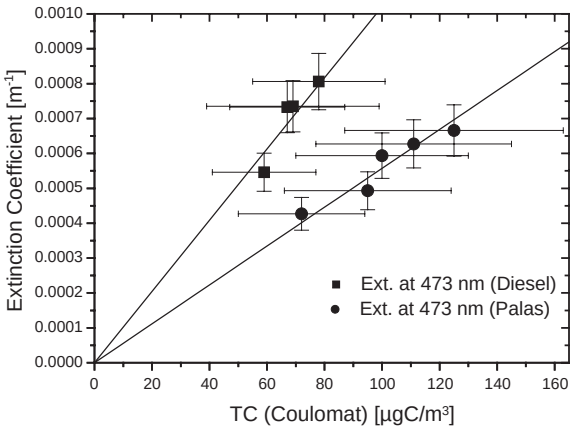

Fig. 9. Comparison of the extinction measured at 473 nm for both soot types with carbon mass concentrations determined by coulometric analysis of quartz filter samples. The slopes of the fitted lines correspond to the specific extinction cross sections of (10.2 ± 0.4) m^2 g^{-1} ($R^2 = 0.904$) and (5.6 ± 0.2) m^2 g^{-1} ($R^2 = 0.918$) determined by Schnaiter et al. (2003) for Diesel and "Palas" soot, respectively.

instrument increased by 43%, while the AE30 signal increased by 66% upon coating as already shown for Diesel soot. For details see the companion paper by Weingartner et al. (2003). Schnaiter et al. (2003) also reported an enhancement of the absorption cross section of about 35% upon coating. The addition of 500 ppb ozone caused the photoemission signal to decrease dramatically by about a factor of 3, confirming the effect observed in experiment no. 7. The remaining signal was rapidly quenched after the addition of α-pinene due to particle coating. The coating increased the TC mass by slightly more than the expected amount of ~42 µg m^{-3}, as discussed above.

In experiment no. 10, α-pinene was added to 500 ppb ozone in aerosol-free air, giving rise to new particle formation (cf. Saathoff et al., 2003a). As shown in Table 1c, analysis of a filter sample collected after the SOA formation event yielded (85 ± 26) µg m^{-3} TC, again significantly more than the estimated carbon yield of 42 µg m^{-3}. After 10 h, the TC mass had decreased to (49 ± 15) µg m^{-3}. Like in previous experiments this decrease is partially due to dilution, SOA loss due to diffusion and sedimentation.

3.4. Comparison of selected carbon measurement methods

The main goal of this campaign was a comprehensive characterisation of Diesel soot aerosol in comparison with "pure" carbon aerosol from a spark discharge generator ("Palas" soot). For this purpose, different instruments were used simultaneously to measure various properties of these aerosols on time scales of up to 2 days, under carefully controlled chamber conditions. As a by-product of this measurement strategy, redundant information was obtained about the strengths and shortcomings of direct methods and other more indirect methods for carbon mass determinations.

Fig. 9 shows correlations between TC mass (determined by combustion of quartz fibre filters followed by coulometric titration of the evolved CO_2) and optical extinction for pure Diesel soot and pure "Palas" carbon aerosols at 473 nm. As discussed in more detail by Schnaiter et al. (2003), the

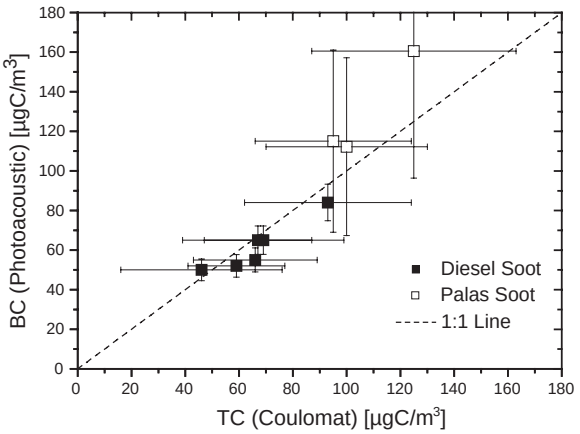

Fig. 10. Comparison of the carbon mass concentrations determined by photoacoustic measurement with those determined by coulometric analysis of quartz filter samples. For this analysis the specific absorption cross sections of (5.4 ± 0.6) m^2 g^{-1} (Diesel) and (1.9 ± 0.8) m^2 g^{-1} ("Palas") determined by Schnaiter et al. (2003) for 680 nm were used.

mass-specific optical properties of Diesel and "Palas" soot are quite different but well reproducible. These differences are largely (but not exclusively) due to the much lower EC content of "Palas" soot, which may be used as a proxy of the BC content. Furthermore, they remain nearly unaffected by particle growth due to coagulation, but are extremely sensitive to coating with SOA. Extinction can thus be used to monitor relative TC mass variations of pure Diesel or "Palas" soot aerosols, but only in the absence of other aerosols and/or coatings.

As detailed in the experimental section, the photoacoustic instrument had been pre-calibrated at the Institute of Hydrochemistry in Munich with "Palas" soot from a different generator. The TC mass-specific absorption cross section deduced from the work done in Munich (2.7 m^2 g^{-1}, Krämer et al., 2001) is about 30% larger than the value determined by Schnaiter et al. (2003). The difference is most probably due to different operating conditions of the "Palas" soot generators used in Munich and at FZK. Additional experiments to investigate and clarify these differences are in preparation. The calibration factors used in this work to determine the photoacoustic BC data displayed in tables and figures are based on the TC mass-specific absorption cross sections of (1.9 ± 0.8) and (5.4 ± 0.6) m^2 g^{-1} for "Palas" and Diesel soot, respectively, at 680 nm, which were obtained by interpolating between the optical measurements of Schnaiter et al. (2003). For Diesel soot, good agreement was found between photoacoustic measurements and TC and EC determinations based on filter samples, as evidenced by the data in Table 1 and the filled squares in Fig. 10. For "Palas" soot, the photoacoustic BC values based on an absorption cross section of 1.9 m^2 g^{-1} are about 20% higher but still within the error limits of the filter based TC determination, as evidenced by the data in Table 1 and the open squares in Fig. 10. With an absorption cross section of 2.7 m^2 g^{-1} as determined by Krämer et al. (2001) they would be about 10% lower.

As already mentioned in previous sections, the total aerosol mass concentrations determined with the betameter systematically exceeded the sum of TC/SOA/ ammonium sulphate mass concentrations. This is shown more clearly by plotting all betameter signals versus the simultaneously measured total aerosol masses (Fig. 11). The slope of the least-squares fit through the origin implies that the

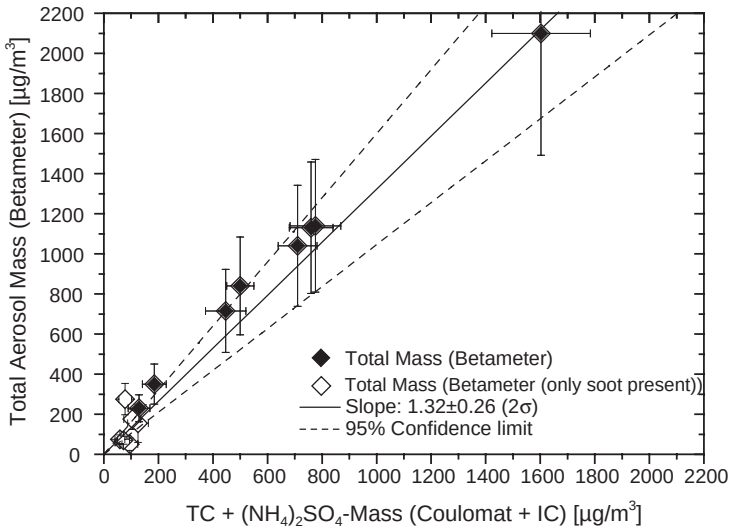

Fig. 11. Comparison of the total aerosol mass determined with the betameter with the sum of carbon and $(NH_4)_2SO_4$ mass concentrations determined by coulometric and ion chromatographic analysis of filter samples ($R^2 = 0.829$).

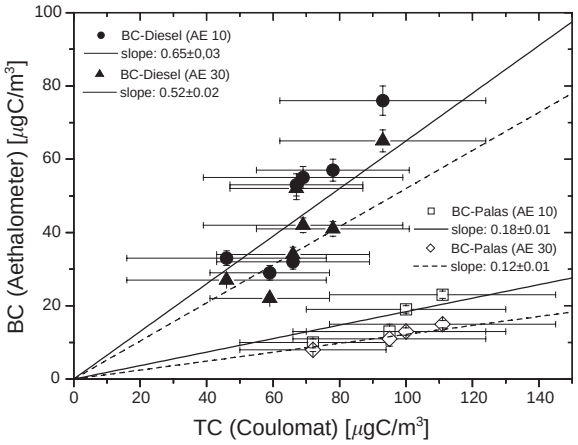

Fig. 12. Comparison of the black carbon mass concentrations determined with both aethalometers for Diesel soot (R^2=0.601 and 0.545) and spark generated "Palas" soot ($R^2 = 0.948$ and 0.994) with the carbon mass concentrations determined by coulometric analysis (TC) of quartz filter samples.

calibration factor provided by the manufacturer should be divided by 1.32 ± 0.26 to obtain correct aerosol mass concentrations. A possible cause for part of this discrepancy may be the remaining water content of the $(NH_4)_2SO_4$ particles.

Correlations between BC masses determined by the AE 10 and AE 30 aethalometers and coulometry-based TC masses are shown for Diesel soot and "Palas" soot in Fig. 12. The slopes of the least-squares fits for Diesel soot are lower than expected because the used specific attenuation cross

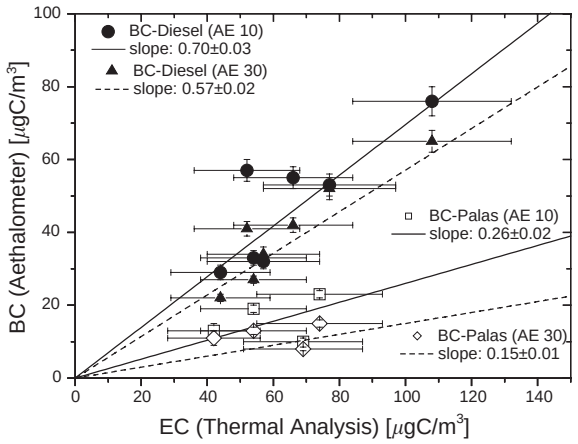

Fig. 13. Comparison of the black carbon mass concentrations determined with both aethalometers for Diesel soot (R^2=0.639 and 0.829) and spark generated "Palas" soot (R^2=0.023 and 0.035) with the carbon mass concentrations determined by thermal analysis (EC) of quartz filter samples.

sections were too high for these types of aerosols. Although only a limited number of data are available for "Palas" soot, the slopes in Fig. 12 indicate a much smaller BC content of "Palas" soot. The correlations between BC masses and EC masses are shown for Diesel soot and "Palas" soot in Fig. 13. The slopes of the least-squares fits for Diesel soot are not in agreement with the assumption BC $\cong$ EC, for the same reason as discussed for Fig. 12. For "Palas" soot, the slopes in Fig. 13 are even much lower. To calculate EC values for these types of particles from the aethalometer measurements cross sections of $16.6 \times 57\%$ for AE30 (Diesel soot), $16.6 \times 15\%$ for AE30 ("Palas" soot), $19 \times 70\%$ for AE10 (Diesel soot), and $19 \times 26\%$ m^2 g^{-1} for AE10 ("Palas" soot), respectively, may be used. This is not surprising since BC and EC contents are based on operational definitions, which are not directly related to meaningful physical or chemical properties. These conclusions are corroborated by a more detailed comparison study of the optical properties of Diesel and "Palas" soot aerosols by Schnaiter et al. (2003).

4. Conclusions

A reasonable agreement was found between direct (i.e. filter based) TC mass analysis, and other more indirect techniques like measurements of optical extinction at 473 nm, and photoacoustic detection. The indirect methods are particularly useful for comparison with model calculations, because measurements can be made continuously or nearly continuously, in contrast to the time and sample air consuming filter based techniques. By means of COSIMA model calculations it was confirmed that the photoelectric current measurements with the photoemission instrument are better correlated with the accessible surface area concentration of soot aerosol than with its mass concentration. Furthermore, the photoelectric signal is strongly reduced by surface reactions with ozone, and is essentially quenched when the particles are coated with SOA mass. This implies that care must be exercised in using the photoemission signal as a proxy for carbon mass concentration.

Furthermore, the optically based techniques require significantly different calibration factors for pure Diesel soot and pure "Palas" aerosols because their optical properties are different, even if referred to EC mass concentration. The approximate relation BC $\cong$ EC for Diesel soot is only valid if correct specific attenuation cross sections are used, e.g. after calibration with an appropriate reference method. While BC measurements by aethalometry and photoacoustics were not significantly affected by the presence of externally mixed non-absorbing aerosol components (e.g. ammonium sulphate), their presence does strongly interfere with extinction measurements. Internal mixtures with non-absorbing aerosol (e.g. secondary organics) affect both.

Acknowledgements

We acknowledge financial support by BMBF under grant (AFS 07AF209) and valuable technical support by Elisabeth Kranz, Georg Scheurig, Rainer Buschbacher, Vincent Lavanchy, and Niklaus Streit.

References

Arens, F., Gutzwiller, L., Baltensperger, U., Gäggeler, H. W., & Ammann, M. (2001). Heterogeneous reaction of NO_2 on diesel soot particles. *Environmental Science and Technology*, *35*, 2191–2199.

Baltensperger, U., Streit, N., Weingartner, E., Nyeki, S., Prévôt, A. S. H., Van Dingenen, R., Virkkula, A., Putaud, J. P., Even, A., ten Brink, H., Blatter, A., Neftel, A., & Gäggeler, H. W. (2002). Urban and rural aerosol characterization of summer smog events during the PIPAPO field campaign in Milan, Italy. *Journal of Geophysical Research*, *107*, 10.1029/2001JD001292.

Baltensperger, U., Weingartner, E., Burtscher, H., & Keskinen, J. (2001). Dynamic mass and surface area measurements. In K. Willeke, P. A. Baron (Eds.), Aerosol measurement: Principles, techniques and applications (2nd ed.), (pp. 387–418). New York: Wiley.

Birch, M. E., & Cary, R. A. (1996). Elemental carbon-based method for monitoring occupational exposures to particulate diesel exhaust. *Aerosol Science and Technology*, *25*, 221–241.

Bukowiecki, N., Kittelson, D. B., Watts, W. F., Burtscher, H., Weingartner, E., & Baltensperger, U. (2002). Real-time characterization of ultrafine and accumulation mode particles in ambient combustion aerosols. *Journal of Aerosol Science*, *33*, 1139–1154.

Burtscher, H. (1992). Measurement and characteristics of combustion aerosols with special consideration of photoelectric charging and charging by flame ions. *Journal of Aerosol Science*, *23*, 549–595.

Burtscher, H., Niessner, R., & Schmidt-Ott, A. (1984). In-situ analysis of coated particles. In B. Liu, D. Pui, & H. Fissan (Eds.), Aerosols, (pp. 436–438). New York: Elsevier.

Burtscher, H., & Siegmann, H. C. (1994). Monitoring PAH-emissions from combustion processes by photoelectric charging. *Combustion Science and Technology*, *101*, 327–332.

Cachier, H., Bremond, M.-P., & Buat-Ménard, P. (1989). Determination of atmospheric soot carbon with a simple thermal method. *Tellus*, *41B*, 379–390.

Chow, J. C., Watson, J. G., Pritchett, L. C., Pierson, W. R., Fraszier, C. A., & Purcell, R. G. (1993). The DRI thermal/optical reflectance carbon analysis system: Description, evaluation and applications in U.S. air quality studies. *Atmospheric Environment*, *27A*, 1185–1201.

Cooke, W. F., Liousse, C., Cachier, H., & Feichter, J. (1999). Construction of a $1^\circ \times 1^\circ$ fossil fuel emission data set for carbonaceous aerosol and implementation and radiative impact in the ECHAM4 model. *Journal of Geophysical Research*, *104*, 22137–22162.

Cooke, W. F., & Wilson, J. J. N. (1996). A global black carbon aerosol model. *Journal of Geophysical Research*, *101*, 19395–19409.

Dahmann, D., Mosimann, T., & Matter, U. (2000). Validation of online sensors for monitoring occupational exposures from diesel engines. *Journal of Aerosol Science*, *31* (Suppl. 1), S21–S22.

Griffin, R. J., Cocker III, D. R., Flagan, R. C., & Seinfeld, J. H. (1999). Organic aerosol formation from the oxidation of biogenic hydrocarbons. *Journal of Geophysical Research*, *104*, 3555–3567.

Hansen, W. N., & Hansen, G. J. (2001). Standard reference surfaces for work function measurements in air. *Surface Science*, *481*, 172–184.

Hansen, A. D. A., & Novakov, T. (1990). Real-time measurement of aerosol black carbon during the carbonaceous species methods comparison study. *Aerosol Science and Technology*, *12*, 194–199.

Hitzenberger, R., Jennings, S. G., Larson, S. M., Dillner, A., Cachier, H., Galambos, Z., Rouc, A., & Spain, T. G. (1999). Intercomparison of measurement methods for black carbon aerosols. *Atmospheric Environment*, *33*, 2823–2833.

Hüglin, C. H., Gaegauf, C. H., Künzel, S., & Burtscher, H. (1997). Characterization of wood combustion particles: Morphology, mobility, and photoelectric activity. *Environmental Science and Technology*, *31*, 3439–3447.

Intergovernmental Panel on Climate Change (IPCC) (2001). In J. T. Houghton, Y. Ding, D. J. Griggs, M. Noguer, P. J. van der Linden, & D. Xiaosu (Eds.), Contribution of working group I to the third assessment report: Climate change 2001: The scientific basis. Cambridge: Cambridge University Press.

Krämer, L., Bozoki, Z., & Niessner, R. (2001). Characterisation of a mobile photoacoustic sensor for atmospheric black carbon monitoring. *Analytical Science*, *17*, S563–S566.

Lavanchy, V. M. H., Gäggeler, H. W., Nyeki, S., & Baltensperger, U. (1999a). Elemental carbon (EC) and black carbon (BC) measurement with a thermal method and an aethalometer at the high-alpine research station Jungfraujoch. *Atmospheric Environment*, *33*, 2759–2769.

Lavanchy, V. M. H., Gäggeler, H. W., Schotterer, U., Schwikowski, M., & Baltensperger, U. (1999b). Historical record of carbonaceous particle concentrations from a European high-alpine glacier (Colle Gnifetti, Switzerland). *Journal of Geophysical Research*, *104*, 21227–21236.

Lide, R. L. (Ed.) (1998). CRC Handbook of chemistry and physics. (79th ed.). Boca Raton, FL: CRC Press.

Liousse, C., Cachier, H., & Jennings, S. G. (1993). Optical and thermal measurements of black carbon aerosol content in different environments: Variation of the specific attenuation cross-section, Sigma (σ). *Atmospheric Environment*, *27A*, 1203–1211.

Liousse, C., Penner, J. E., Chuang, C., Walton, J. J., Eddleman, H., & Cachier, H. (1996). A global three-dimensional model study of carbonaceous aerosols. *Journal of Geophysical Research*, *101*, 19411–19432.

Matter, U., Siegmann, H. C., & Burtscher, H. (1999). Dynamic field measurement of submicron particles from diesel engines. *Environmental Science and Technology*, *33*, 1946–1952.

Moosmüller, H., Arnott, W. P., Rogers, C. F., Bowen, J. L., Gillies, J. A., Pierson, W. R., Collins, J. F., Durbin, T. D., & Norbeck, J. M. (2001). Time resolved characterisation of diesel particulate emissions. 2. Instruments for elemental and organic carbon measurements. *Environmental Science and Technology*, *35*, 1935–1942.

Moosmüller, H., Arnott, W. P., Rogers, C. F., Chow, J. C., Frazier, C. A., Sherman, L. E., & Dietrich, D. L. (1998). Photoacoustic and filter measurements related to aerosol light absorption during the Northern Front Range Air Quality Study (Colorado 1996/1997). *Journal of Geophysical Research*, *103*, 28149–28157.

Naumann, K.-H. (2003). COSIMA—a computer program simulating the dynamics of fractal aerosols. *Journal of Aerosol Science*, *34*, 1371–1397.

Niessner, R. (1986). The chemical response of the Photoelectric Aerosol Sensor to different aerosol systems. *Journal of Aerosol Science*, *17*, 705–714.

Novakov, T., Corrigan, C. E., Penner, J. E., Chuang, C. C., Rosario, O., & Bracero, O. L. M. (1997). Organic aerosols in the Caribbean trade winds: A natural source? *Journal of Geophysical Research*, *102*, 21307–21313.

Penner, J. E., & Novakov, T. (1996). Carbonaceous particles in the atmosphere: A historical perspective to the fifth international conference on carbonaceous particles in the atmosphere. *Journal of Geophysical Research*, *101*, 19373–19378.

Petzold, A., & Niessner, R. (1995). Method comparison study on soot-selective techniques. *Mikrochimica Acta*, *117*, 215–237.

Pöschl, U., Letzel, T., Schauer, C., & Niessner, R. (2001). Interaction of ozone and water vapor with spark discharge soot aerosol particles coated with benzo[a]pyrene: O_3 and H_2O adsorption, benzo[a]pyrene degradation, and atmospheric implications. *Journal of Physical Chemistry A*, *105*(16), 4029–4041.

Raes, F., Van Dingenen, R., Vignati, E., Wilson, J., Putaud, J.-P., Seinfeld, J. H., & Adams, P. (2000). Formation and cycling of aerosols in the global troposphere. *Atmospheric Environment*, *34*, 4215–4240.

Saathoff, H., Möhler, O., Naumann, K.-H., Schnaiter, M., Schöck, W., Schurath, U., Weingartner, E., Gysel, M., & Baltensperger, U. (2003a). Coating of soot and $(NH_4)_2SO_4$ particles by ozonolysis of α-pinene. *Journal of Aerosol Science*, *34*, 1297–1321.

Saathoff, H., Möhler, O., Schurath, U., Kamm, S., Dippel, B., & Mihelcic, D. (2003b). The AIDA soot aerosol characterisation campaign 1999. *Journal of Aerosol Science*, *34*, 1277–1296.

Schmid, H., Laskus, L., Abraham, H. J., Baltensperger, U., Lavanchy, V., Bizjak, M., Burba, P., Chachier, H., Crow, D., Chow, J., Gnauk, T., Even, A., ten Brink, H. M., Giesen, K.-P., Hitzenberger, R., Hüglin, C., Maenhaut, W., Pio, C., Carvalho, A., Putaud, J.-P., Toom-Sauntry, D., & Puxbaum, H. (2001). Results of the "carbon conference" international aerosol carbon round robin test stage I. *Atmospheric Environment*, *35*, 2111–2121.

Schnaiter, M., Horvath, H., Möhler, O., Naumann, K.-H., Saathoff, H., & Schöck, O. W. (2003). UV-VIS-NIR spectral optical properties of soot and soot-containing aerosols. *Journal of Aerosol Science*, *34*, 1421–1444.

Toon, O. B., Pollack, J. B., & Khare, B. N. (1976). The optical constants of several atmospheric aerosol species: Ammonium sulfate, aluminium oxide, and sodium chloride. *Journal of Geophysical Research*, *81*, 5733–5748.

VDI (1987). Particulate matter measurement; Measurement of mass concentration in ambient air; Filter method; Automated Filter Device FH_62_I. VDI-Handbuch Reinhaltung der Luft Teil 4, guideline 2463, Blatt 5.

VDI (1996). Measurement of soot (Immission)—chemical analysis of elemental carbon by extraction and thermal desorption of organic carbon. VDI/DIN-Handbuch Reinhaltung der Luft, Band 4, VDI 2465 Part 1. Beuth, Berlin.

VDI (1999). Measurement of soot (Ambient air)—thermographic determination of elemental carbon after thermal desorption of organic carbon. VDI/DIN-Handbuch Reinhaltung der Luft, Band 4, VDI 2465 Part 1. Beuth, Berlin.

Weingartner, E., Saathoff, H., Schnaiter, M., Streit, N., Bitnar, B., & Baltensperger, B. (2003). Absorption of light by soot particles: Determination of the absorption coefficient by means of aethalometers. *Journal of Aerosol Science*, *34*, 1445–1463.

Wentzel, M., Gorzawski, H., Naumann, K.-H., Saathoff, H., & Weinsbruch, S. (2003). Transmission electron microscopical and aerosol dynamical characterization of soot and ammonium sulfate/soot mixtures. *Journal of Aerosol Science*, *34*, 1347–1370.

Yu, J., Cocker III, D. R., Griffin, R. J., Flagan, R. C., & Seinfeld, J. H. (1999). Gas-phase ozone oxidation of monoterpenes: Gaseous and particulate products. *Journal of Atmospheric Chemistry*, *34*, 207–258.